Available online at www.sciencedirect.com
ScienceDirect
Bioorganic & Medicinal Chemistry Letters 17 (2007) 6280–6285
Bioorganic & Medicinal Chemistry Letters

Synthesis and evaluation of substituted benzoisoquinolinones as potent inhibitors of Chk1 kinase

Robert M. Garbaccio,[a,*] Shaei Huang,[a] Edward S. Tasber,[a] Mark E. Fraley,[a] Youwei Yan,[b] Sanjeev Munshi,[b] Mari Ikuta,[b] Lawrence Kuo,[b] Constanine Kreatsoulas,[a] Steve Stirdivant,[c] Bob Drakas,[c] Keith Rickert,[c] Eileen S. Walsh,[c] Kelly A. Hamilton,[c] Carolyn A. Buser,[c] James Hardwick,[c] Xianzhi Mao,[c] Stephen C. Beck,[c] Marc T. Abrams,[c] Weikang Tao,[c] Rob Lobell,[c] Laura Sepp-Lorenzino[c] and George D. Hartman[a]

[a]*Department of Medicinal Chemistry, Merck Research Laboratories, West Point, PA 19486, USA*
[b]*Department of Structural Biology, Merck Research Laboratories, West Point, PA 19486, USA*
[c]*Department of Cancer Research, Merck Research Laboratories, West Point, PA 19486, USA*

Received 1 August 2007; revised 28 August 2007; accepted 4 September 2007
Available online 7 September 2007

Abstract—From HTS lead **1**, a novel benzoisoquinolinone class of ATP-competitive Chk1 inhibitors was devised and synthesized via a photochemical route. Using X-ray crystallography as a guide, potency was rapidly enhanced through the installation of a tethered basic amine designed to interact with an acidic residue (Glu91) in the enzyme pocket. Further SAR was explored at the solvent front and near to the H1 pocket and resulted in the discovery of low MW, sub-nanomolar inhibitors of Chk1.

Despite their inherent toxicity, DNA damaging agents continue to remain central in clinical cancer chemotherapy. Therefore, strategies directed at improving their therapeutic index are warranted. Following DNA damage, normal cells arrest and attempt repair at the cell cycle checkpoints G1 and S, via the tumor suppressor protein p53, and at G2 and S via the checkpoint kinase Chk1.[1–3] Tumor cells, however, are often deficient in p53 function (estimated 50–70% of all cancers) and thus, must rely on Chk1 to induce arrest for survival. These p53-deficient cancers should be more vulnerable to Chk1 inhibition, leading to abrogation of DNA-damage-induced arrest, premature progression into mitosis and resulting in mitotic catastrophe and apoptosis. To summarize, abrogation of the S and G2 checkpoints should sensitize p53-deficient cancer cells to DNA damaging agents without enhancing toxicity toward normal proliferating cells. As such, Chk1 inhibitors[4] have the potential to widen the therapeutic window for clinically-utilized DNA damaging agents in p53 deficient tumors.

This effort initiated with the tetracyclic lead (**1**) that was derived from an earlier Jak kinase effort at Merck.[5] An X-ray crystal structure was obtained for **1** and revealed the expected interaction of the hydrogen bond donor/acceptor pair of the pyridone with the kinase backbone in the hinge region of the ATP active site. The 3-pyridyl analog **3** demonstrated that some enhancement in potency might be obtained by extension of a basic amine in the region of the Glu91 and Glu134 residues in the ATP pocket of Chk1.

One concern in this structure was the presence of the imidazole group (calcd p*K*a for benzimidazole ~5.8) which contributed elevated polar surface area (PSA) while likely not contributing to potency. Earlier studies suggested that elevated PSA and multiple basic sites in Chk1 inhibitors were detrimental to cell potency.[6] In keeping with these observations, a strategy emerged to remove the imidazole from **1**, therein producing a novel benzoisoquinolinone core that had the potential to be elaborated further to make key potency-enhancing contacts (Fig. 1).

Keywords: Chk1 kinase; Chek1 kinase; Kinases; Photochemistry; Benzoisoquinolinones; PSA; DNA damaging agents; Mitotic arrest; Checkpoint escape; p53-Deficient cancer; Cancer; Apoptosis.
* Corresponding author. Tel.: +1 215 652 5391; fax: +1 215 652 6345; e-mail: robert_garbaccio@merck.com

0960-894X/$ - see front matter
doi:10.1016/j.bmcl.2007.09.007

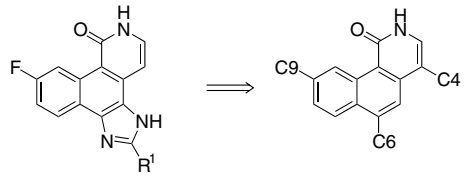

Cmpd	R^1	Chk1 IC_{50}
1	H	610 nM
2	Ph	1080 nM
3	3-pyridine	110 nM

Benzoisoquinolinones

- reduced core polarity
- improve potency
- explore SAR

Figure 1. HTS lead **1** and preliminary SAR along with the proposed benzoisoquinolinone core.

Further analysis of the X-ray structure of **1** suggested the placement of a basic amine approximately 4–5 angstroms from C6 of the benzoisoquinolinone core would interact with the acidic residue Glu91 and would result in greater potency. Accordingly, it was decided to devise a general synthetic route that could access both an ethylamine and propylamine substitution at C6 from a common starting material (Schemes 1 and 2).

Stobbe-condensation of substituted benzonitriles **4** with pyridine-4-carboxaldehyde **5** yielded the *E*-azastillbenes **6** in moderate yield.[7] A key step in this synthesis was the oxidative photocyclization of **6** to the azaphenanthrene **7**. While slow and somewhat low-yielding (30%), this reaction was run reproducibly on 80 g scale, used O_2(g) as an oxidant, and did not require high dilution. In addition, upon concentration the pure product **7** precipitated from the reaction mixture and was easily isolated. The presence of *t*-BuOH was found to accelerate the reaction consistent with an earlier observation.[8]

Elaboration of the C6–CN group into primary alcohol (**9**) was accomplished in three high-yielding steps: (1) hydrolysis to the acid, (2) Fisher esterification to the ester and (3) reduction using LAH. The alcohol was then oxidized to the aldehyde **10**. Despite efforts to shorten the sequence from **7** to **10**, no simplified route was identified. Importantly, however, no chromatography was required for these first 6 steps. Homologation of the aldehyde **10** to the acrylonitrile **11** and subsequent 1,4-reduction with $NaBH_4$ gave the C6-ethylnitrile **12**. At this stage, N-oxidation with *m*-CPBA and regioselective rearrangement to the pyridone provided benzoisoquinolinone **14**. The regioselectivity of this transformation is rationalized by resonance arguments that maintain the aromaticity of the naphthalene core. After considerable experimentation, it was found that LAH provided the optimal conditions for reduction of the nitrile to the primary amine **15**.

In the sequence for which X = Br, Suzuki couplings with various boronic acids allowed for exploration of the C9 SAR (results reported below).

Alternatively, the intermediate alcohol **9** could be directed toward the formation of the C6-ethylamine benzoisoquinolinones **22** (Scheme 2). Again, regioselective conversion to the pyridone **18** was strictly observed.

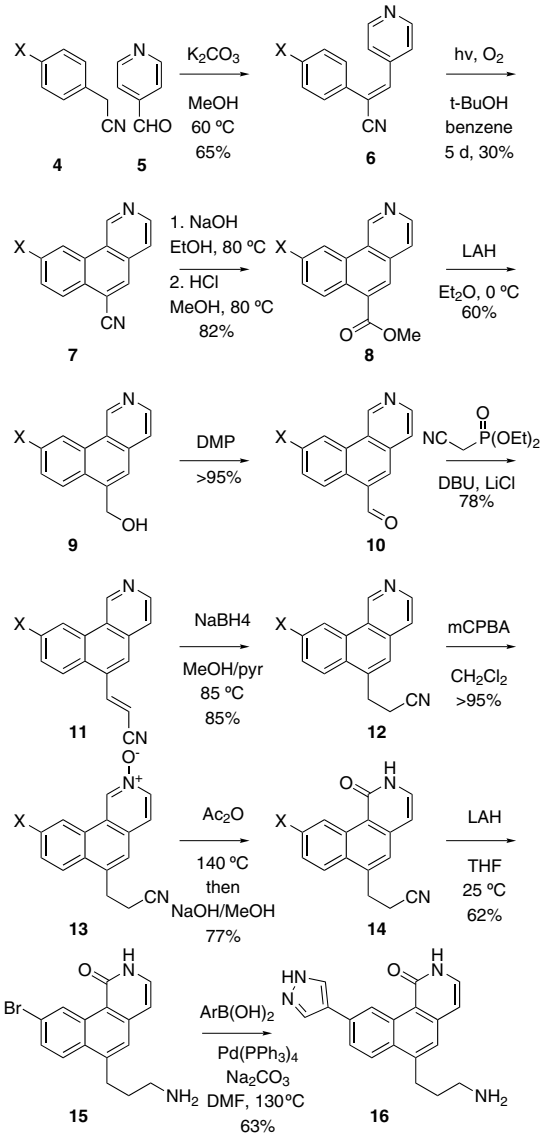

Scheme 1. Photochemical route to C6-propylamine benzoisoquinolinones.

Conversion to the primary mesylate **19** was followed by direct displacement with NaCN to provide the nitrile **20**. Here, LAH was found to lead to significant decomposition whereas BH_3–THF provided clean reduction to the ethylamine **21**. Again, for the C9–Br, metal-mediated coupling reactions allowed for exploration at C9.

The final vector that was explored in this benzoisoquinolinone core emanated from the C4-position. Substitution at C4 would extend into the H1 pocket[9] and surrounding hydrophobic space that is left unused by HTS lead **1**. The reactivity of the pyridone moiety (even in the presence of the pyrazole) in these benzoisoquinolinones allowed for late-stage bromination at C4 and further Suzuki-couplings to determine the effect of extending substitution into that region (Scheme 3).

These benzoisoquinolinone inhibitors proved to be excellent structural surrogates for the HTS lead **1** and through this versatile synthetic route, superior enzymatic and

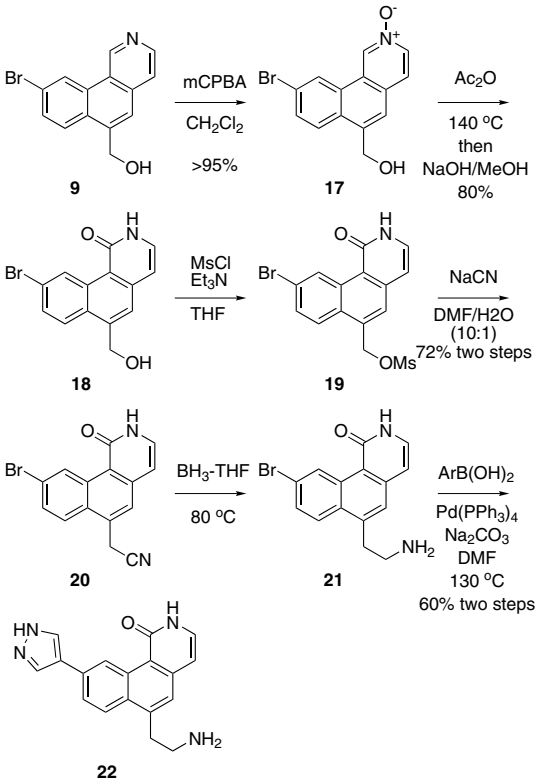

Scheme 2. Conversion of intermediate **9** into C6-ethylamine benzoisoquinolinones.

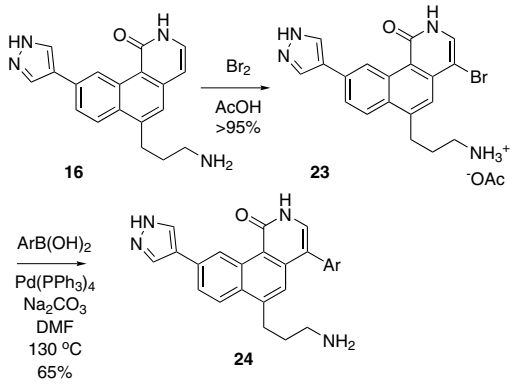

Scheme 3. C4 bromination and Suzuki couplings.

cellular-potency were achieved in structures with low molecular weight (M_W <300). In Table 1, a comparison of C6 substitutions establishes that the benzoisoquinolinone core is potent and that both the ethyl- and propyl-linked amines provide excellent potency enhancement. The core itself with a C9–Cl group (**25**) gave an IC_{50} = 580 nM against Chk1 confirming that the imidazole was not needed for potency.[10] Various neutral substitutions (**26–31**) did not greatly alter potency, however, both the propyl amine (**32** and **33**) and the ethyl amine (**34** and **35**) provided approximately 30-fold improvements in potency relative to **25**. This potency enhancement is lost completely by replacement of the amine with an alcohol (**36**), and is even diminished with mono- (**38**) and bismethylation (**39**) of the amine. These observations are consistent with an ionic interaction between a

Table 1. Ethyl- and propylamine benzoisoquinolinones

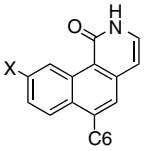

Compound	X	C6	Chek1 IC_{50}[a] (nM)
25	Cl	H	580
26	Cl	CN	1060
27	Br	CN	400
28	Cl	CO_2Me	360
29	Br	CO_2Me	300
30	Cl	$(CH_2)_2CN$	510
31	Br	$(CH_2)_2CN$	420
32	Cl	$(CH_2)_3NH_2$	12
33	Br	$(CH_2)_3NH_2$	17
34	Cl	$(CH_2)_2NH_2$	11
35	Br	$(CH_2)_2NH_2$	3
36	Br	CH_2OH	440
37	Br	$(CH_2)_2OH$	780
38	Br	$(CH_2)_2NHMe$	44
39	Br	$(CH_2)_2NMe_2$	130

[a] Run at K_m for ATP (0.1 mm).

protonated primary amine and Glu91 (detailed analysis of an X-ray structure presented below).

With either a propyl- or ethylamine at C6, exploration of C9 commenced (Table 2). Substitutions at C9 are directed toward the solvent front of the Chk1 ATP-binding pocket and those substitutions that would form beneficial interactions in this environment while minimizing molecular PSA <100 Å^2 were sought out to maximize cellular potency. These inhibitors were tested against the enzyme and also in a cell-based checkpoint escape assay that measures the ability of a Chk1 inhibitor to release H1299 tumor cells from camptothecin-induced cell cycle arrest.[11,12] The C9–Br derivative **32** or Cl derivative **33** gave approximately a 7-fold improvement in potency relative to the unsubstituted derivative **40**. Substitution to the nitrile **41** or the corresponding amide **42** resulted in minimal intrinsic potency change, but diminished cellular potency (note PSA increase).[13] Conversion to the 3-pyrazole or 4-pyrazole (**16, 22, 43–44**) gave a further 3- to 4-fold potency increase and provided compounds with excellent cell potency. Suprisingly, the log P value for **16** was measured to be 0.0 and yet it appears to have sufficient cell permeability. C9-Pyrroles **45** and **46** were sub-nanomolar inhibitors in this series with exceptional cell potency. The hydrogen-bond donor ability of these pyrazoles and pyrroles may contribute to potency as the methylated pyrazole **47** was 3-fold less potent. Inhibitors **48–50** were designed to interact with solvent, but their additional basic amine and increased PSA appeared to have a negative impact on cell potency.[6] Due to potential stability and metabolic activation issues seen with pyrroles, the C6-pyrazole (as in **16** and **22**) was selected as the preferred substitution.

Benzoisoquinolinone **16** was brominated selectively at C4 and a library of Suzuki reactions was conducted to

Table 2. C9-substituted benzoisoquinolinones

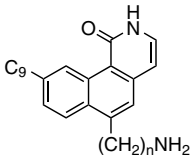

Compound	n	C9	Chek1 IC_{50}[a] (nM)	Cell EC_{50} (nM)	PSA (Å^2)
40	3	H	98	n.t.	62
32	3	CL	12	230	61
33	3	Br	17	310	61
41	3	CN	25	2200	88
42	3	$CONH_2$	11	>10,000	107
22	2		3.0	79	96
16	3		3.5	64	96
43	2		2.5	100	95
44	3		4.3	150	93
45	2		0.5	14	75
46	3		2.4	44	75
47	3		9.2	957	82
48	3	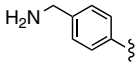	6.5	1085	90
49	2	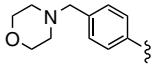	0.6	130	79
50	3	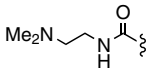	2.0	>10,000	95

[a] Run at K_m for ATP (0.1 mM).

complete our SAR assessment in the H1 pocket. While some potency improvements were seen in terms of enzymatic activity, these improvements typically did not translate into elevated cell potency. At the risk of increasing molecular weight, it was found that considerable steric bulk could be accommodated at this position. The bromide **23** was more potent against Chk1 than **16** but less potent in the checkpoint escape cellular assay. Among the numerous groups employed, the phenols **54**–**56** and the chlorides **59** and **61** did increase enzymatic potency, but the expected increase in cell potency was not realized relative to **16**. In the case of the phenols **53**–**55**, PSA is increased, and it is possible that this correlates with some decreased permeability (relative to **16**). For the aryl halides **56**–**62** it is not clear why cell potency decreases relative to **16**. Lastly, the potency with the combination of the *ortho*- and *para*-Cl substitution was not additive in **62**. The larger molecular weight of the compounds in Table 3 (>400) may contribute to the lack of improvement in cellular potency for these C4-substituted inhibitors.

The ability of a Chek1 inhibitor to sensitize a tumor cell line to apoptosis and cell death was examined in a

Table 3. C4-substituted benzoisoquinolinones

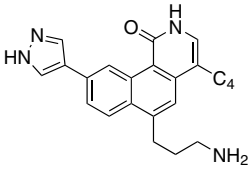

Compound	C4	Chek1 IC_{50}[a] (nM)	Cell EC_{50} (nM)	PSA (Å^2)
16	H	3.5	64	96
23	Br	2.3	140	95
51	$CH{=}CH_2$	3.6	210	97
52	Ph	2.0	140	97
53	2-(OH)–Ph	2.0	230	120
54	3-(OH)–Ph	1.0	67	120
55	4-(OH)–Ph	0.3	47	120
56	2-(F)–Ph	2.6	370	96
57	3-(F)–Ph	3.7	300	96
58	4-(F)–Ph	3.5	370	96
59	2-(Cl)–Ph	0.8	130	97
60	3-(Cl)–Ph	11.5	1050	97
61	4-(Cl)–Ph	1.2	320	97
62	2,4-$(Cl)_2$–Ph	1.2	270	96

[a] Run at K_m for ATP (0.1 mM).

caspase activation assay—a measure of apoptosis.[14] HT29 cells were treated sequentially with camptothecin followed by compound **22**, then assayed for caspase 3 activity. While camptothecin by itself induces some level of caspase activity, addition of increasing concentrations of compound **22** following camptothecin exposure increased the activity over camptothecin alone (Fig. 2). Compound **22** by itself had no effect on caspase activity. The results are consistent with the hypothesis that release of cells from DNA damage checkpoint arrest results in mitotic catastrophe and cell death.

An X-ray crystal structure of the inhibitor-bound complex with Chk1 for compound **54** was obtained and analyzed in order to understand the multiple interactions with the enzyme (Fig. 3).[15] Several key hydrogen bonds are made by this molecule that rationalize the increase in potency afforded by the pyrazole, propylamine, and phenol moeties and help to explain the SAR. First, the

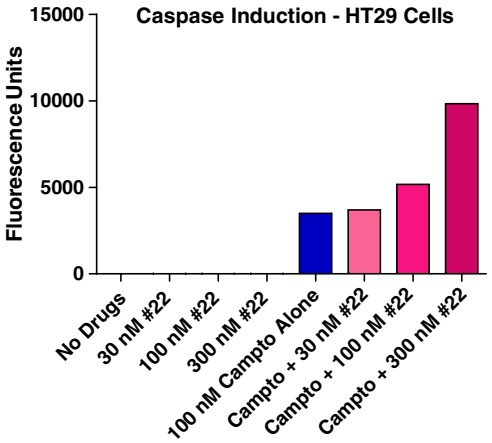

Figure 2. Caspase-induction assay with camptothecin and **22**.

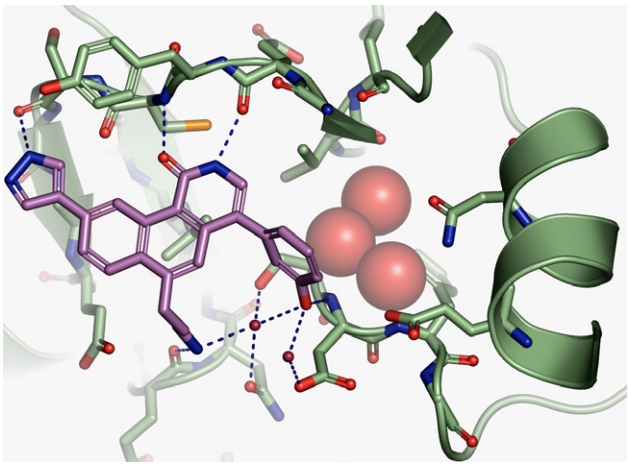

Figure 3. X-ray structure of benzoisoquinolinone **54** bound to Chk1.

pyrazole group makes a hydrogen bond with Ser88 of Chk1. While halogens cannot make this hydrogen bond, Leu20 which lies above the plane of the pyrazole C1 position and the aromatic ring of Tyr86 provides a Van derWaals interaction surface. The propylamine and phenol groups of **54** make numerous hydrogen bonds with protein (both backbone and side chain atoms) and water molecules. Interestingly, the three water molecules which occupy the H1 hydrophobic pocket of Chk1 are not making contacts with the inhibitor (as has been seen in other Chk1: inhibitor structures).[6] It is readily apparent that moving the phenol oxygen to the 4-position (**55**) would allow for hydrogen bonding to one of the three waters in H1 (red spheres in Fig. 3) and to Glu55, a stronger hydrogen bond than that to the backbone.

In summary, a novel benzoisoquinolinone core was designed and developed based on HTS lead **1** following a strategy of minimizing the number of basic amines and the PSA values of target compounds. A versatile photochemical synthetic route was developed that allowed for complete control and combination of substitution at C4, C6, and C9. These efforts were guided by X-ray crystallography that correctly predicted the general potency enhancements observed with both the ethyl- and propylamine substitution at C6. Further exploration revealed that the use of nitrogen-heterocycles at C9 provided Chk1 inhibitors with outstanding potency in both enzymatic and cell based assays. The subtle structural effects in this and other series of Chk1 inhibitors on cellular potency and permeability are not fully understood, but a strategy in which PSA and the number of basic amines is minimized in final inhibitor structures expedited the discovery of this potent, cell-permeable class of Chk1 kinase inhibitors.

Supplementary data

Supplementary data associated with this article can be found, in the online version, at doi:10.1016/j.bmcl.2007.09.007.

References and notes

1. (a) Zhou, B. B.; Bartek, J. *Nat. Rev. Cancer* **2004**, *4*, 1; (b) Bartek, J.; Lukas, J. *Cancer Cell* **2003**, *3*, 421.
2. Kong, N.; Fotouhi, N.; Wovkulioch, P. M.; Roberts, J. *Drug Future* **2003**, *28*, 881.
3. Kawabe, T. *Mol. Cancer Ther.* **2004**, *3*, 513.
4. (a) Prudhomme, M. *Recent Patent Anti-Cancer Drug Dis.* **2006**, *1*, 55; (b) Tao, Z.-F.; Lin, N.-H. *Anti-Cancer Agents in Med. Chem.* **2006**, *6*, 377.
5. (a) Thompson, J. E.; Cubbon, R. M.; Cummings, R. T.; Wicker, L. S.; Frankshun, R.; Cunningham, B. R.; Cameron, P. M.; Meinke, P. T.; Liverton, N.; Weng, Y.; DeMartino, J. A. *Biorg. Med. Chem. Lett.* **2002**, *12*, 1219; (b) Goulet, J. L.; Hong, X.; Sinclair, P. J.; Thompson, J. E.; Cubbon, R. M.; Cummings, R. T. PCT Int. Appl. WO 2003011285, **2003**.
6. Huang, S.; Garbaccio, R. M.; Fraley, M. E.; Steen, J.; Kreatsoulas, C.; Hartman, G.; Stirdivant, S.; Drakas, B.; Rickert, K.; Walsh, E.; Hamilton, K.; Buser, C. A.; Hardwick, J.; Mao, X.; Abrams, M.; Beck, S.; Tao, W.; Lobell, R.; Sepp-Lorenzino, L.; Yan, Y.; Ikuta, M.; Zugay-Murphy, J.; Sardana, V.; Munshi, S.; Kuo, L.; Reilly, M.; Mahan, E. *Biorg. Med. Chem. Lett.* **2006**, *22*, 5907.
7. All compounds were characterized by ^{1}H NMR and high resolution mass spectrometry. For detailed experimental procedures, see patent WO 2007008502.
8. Kumler, P. L.; Dybas, R. A. *J. Org. Chem.* **1970**, *35*, 125.
9. Traxler, P.; Furet, P. *Pharmacol. Ther.* **1999**, *82*, 195.
10. Chk1 inhibitory activity was measured using a homogenous time-resolved fluorescence assay which measures phosphorylation of a biotinylated GSK-3 peptide as described in Barnett, S. et al. *Biochem. J.* **2005**, *385*, 399, For the construct, a naturally occurring exon 10 splice variant of the human Chk1 described in patent application US200502666469(A1), containing primarily the kinase domain, was expressed in baculovirus with a C-terminal 6-histidine tag. The protein was purified on a Ni affinity column and used as it is for kinetic assays, or purified further on Heparin and SEC columns for crystallography. The Chk1 concentration was 0.5 nM and ATP was used at 0.1 mM. IC_{50} values are reported as the averages of at least two independent determinations; standard deviations are within ±25–50% of IC_{50} values.
11. NCI-H1299 lung carcinoma cells were arrested with 16 h treatment of camptothecin, and then treated with Chk1 inhibitors for additional 8 h. Checkpoint escape due to Chk1 inhibition was assessed by measuring the mitotic specific phosphorylation of nucleolin in Chk1 inhibitor treated cells using an antibody coated, bead-based assay. In this assay, total nucleolin is captured on a streptavidin-coated paramagnetic bead coupled with biotinylated nucleolin monoclonal antibody 4E2 (Research Diagnostics, Inc.). Phosphorylated nucleolin is detected by an antibody complex consisting of a phospho-specific nucleolin monoclonal antibody TG3 (Applied NeuroSolutions, Inc.) and a ruthenylated goat anti-mouse IgM antibody labeled with ruthenylation kit (BioVeris Corp). The electrochemiluminescent complex is quantified with BioVeris M-8 Analyzer. The $EC_{50}$of checkpoint escape mediated by Chk1 inhibition was determined with 10-point series diluted Chk1 inhibitor treated tetraplicate cell samples.
12. Note that Chk1 inhibitory activity is measured at K_m for ATP (0.1 mM). In the cell assay, the ATP concentration is

2.0 mM resulting in an inherent 10-fold potency shift between these assays.

13. PSA calculations are done using the method published by Clark in 1999: Clark, D. E. *J. Pharm. Sci.* **1999**, *88*, 807.
14. Caspase activation assay method HT29 cells were seeded in 6-well plates at a density of 5×10^4 cells per well in DMEM media +10% fetal calf serum. When cells reached 50% confluency, 100 nM camptothecin was added in fresh media and incubation continued for 24 h after which the media was again replaced with fresh media containing 30, 100 or 300 nM of compound **22**. After 24 h of exposure to the Chek1 inhibitor, caspase 3 activity in cells was measured using the Caspase 3 Assay Kit (Becton–Dickinson) according to the manufacturer's instructions. Fluorescence was measured on a Spectramax Gemini plate reader (Molecular Devices).
15. Compounds **54** was diffused into pre-formed apo Chek1 crystals by the soaking method. The X-ray diffraction data were collected from this Chk1 inhibitor complex crystals to 1.9 Å resolution with $R_{sym} = 0.051$, and completeness = 99%. The complex structure was refined to an *R*-factor of 0.195. The detailed X-ray diffraction data and refinement statistics are listed under PDB code 2R0U at the protein data bank.